JOURNAL OF SOLID STATE CHEMISTRY 43, 175–180 (1982)

Crystal Field Effects on the Magnetic Behavior of $Yb_2V_2O_7$ and $Tm_2V_2O_7$

LYNNE SODERHOLM,* C. V. STAGER,† AND J. E. GREEDAN*

*Institute for Materials Research and Departments of *Chemistry and †Physics, McMaster University, Hamilton, Ontario L8S 4M1, Canada*

Received December 21, 1981; in final form February 23, 1982

The bulk magnetic behaviors of the pyrochlores $Yb_2V_2O_7$ and $Tm_2V_2O_7$ were investigated. Calculated susceptibilities were adjusted to obtain the best fit to experimental data. A cubic crystal field Hamiltonian was used with $B_4^\circ = -0.633$ and $B_6^\circ = 0.000705$ K for Yb^{3+} and $B_4^\circ = 0.0297$ and $B_6^\circ = 0.000339$ K for Tm^{3+}. The calculated susceptibility for Yb^{3+} was found to be insensitive to the addition of an axial B_2° parameter to the cubic Hamiltonian.

Introduction

There have been several attempts to understand the magnetic behavior of the pyrochlores $(RE)_2V_2O_7$ (RE = Lu, Yb, Tm) since the initial report that $Lu_2V_2O_7$ was simultaneously ferromagnetic and semiconducting (*1*). While $Lu_2V_2O_7$ appears to exhibit basic magnetic properties consistent with ferromagnetic coupling of the V moments, there have been discrepancies in the interpretation of the magnetic behavior of $Yb_2V_2O_7$. The low-temperature magnetization has been interpreted as resulting from the ferromagnetic coupling of the Yb^{3+} and V^{4+} sublattices (*2, 3*), with the low-saturation magnetization attributed to quenching of the Yb^{3+} moment by the crystalline electric field. Low-temperature neutron diffraction data (*3*) were consistent with this interpretation.

Bazuev *et al.* (*1, 2*) reported that the plot of inverse susceptibility for $Yb_2V_2O_7$, from 300 to 77K, had a change of slope at 190K which separated two linear regions. Shinike *et al.* (*4*) also examined $Yb_2V_2O_7$ and reported Curie–Weiss behavior over the same temperature range. A previous investigation by Soderholm *et al.* (*3*) showed a curvature below 190K but the deviation from rectilinear behavior was attributed to crystal field effects.

Two groups investigated the isostructural compound $Yb_2Ti_2O_7$ in which the only magnetic ion is Yb^{3+}. The site symmetry of the RE is D_{3d}, which leads to a crystal field Hamiltonian $\mathcal{H}_{CF} = B_2^0O_2^0 + B_4^0O_4^0 + B_6^0O_6^6 + B_4^3O_4^3 + B_6^3O_6^3 + B_6^6O_6^6$. Dunlap *et al.* (*5*) truncated this Hamiltonian to the axial version

$$\mathcal{H}_{CF} = B_2^0O_2^0 + B_4^0O_4^0$$

to explain the magnetic field dependence of ^{170}Yb Mössbauer spectra. They found a $|\pm\frac{3}{2}>$ ground state with the first excited state, $|\pm\frac{1}{2}>$, at 18K. Townsend and Crossley (*6*) interpreted susceptibility data on the same compound in the range 2–1400K using a cubic crystal field Hamiltonian with an added axial term.

0022-4596/82/080175-06$02.00/0

$$\mathcal{H}_{CF} = B_2^0 O_2^0 - \tfrac{1}{2}B_4^0(O_4^0 - 20\,2^{1/2}O_4^3) + 16/9B_6^0(O_6^0 + 32\,2^{1/2}/4 + O_6^3 + 77/8O_6^6).$$

They found, for the cubic Hamiltonian, a Γ_7 ground state with a first excited state Γ_6 at 1040K. Townsend *et al.* varied the B_2^0 term from zero until it was as large as the B_4^0 term and found that the fit to experimental data was insensitive to the second-order term.

Clearly these two energy level schemes are not consistent. Since the Yb^{3+} ion is in the same environment in both the titanium and vanadium pyrochlores it was felt that the crystal field calculations on $Yb_2V_2O_7$ and $Tm_2V_2O_7$ might prove helpful in resolving this discrepancy as well as in explaining the magnetic properties of the vanadium pyrochlores.

Experimental Method

The pyrochlores were prepared by heating $REVO_4$ in a carefully controlled reducing atmosphere. Details of the preparation and characterization of these compounds may be found elsewhere (*7*). The susceptibility and magnetization data were collected on a nickel-calibrated, vibrating sample magnetometer. Temperatures were measured with a gold–0.07% iron versus chromel thermocouple.

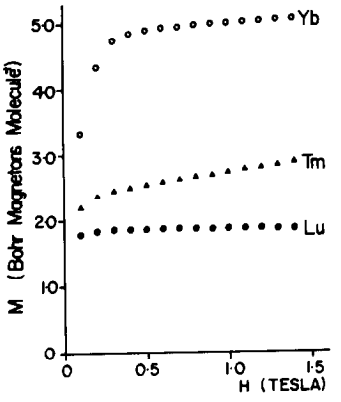

FIG. 1. Magnetic moment versus magnetic field curves at 4K.

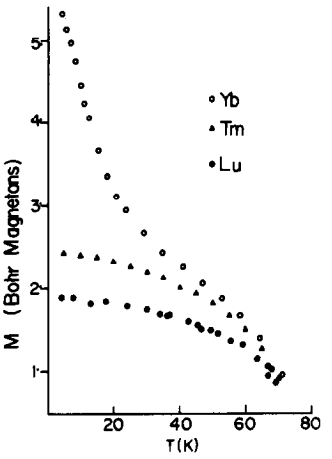

FIG. 2. Magnetic moment, per $(RE)_2V_2O_7$ molecule, versus temperature curves obtained from the M versus H curves.

Experimental Results

Magnetization data as a function of magnetic field were collected for all three compounds at several temperatures below T_c. Representative curves are shown in Fig. 1. The magnetization, $M(T)$, was obtained by fitting the field dependence to the expression

$$M(H,T) = M(T)[1 - A/H] + BH.$$

The resulting values are plotted as a function of temperature in Fig. 2. The saturation magnetizations, at 4K, and critical temperatures are shown in Table I. Also, susceptibility data were recorded from 110–300K for all three compounds.

To examine the contribution to the magnetic properties of the *RE* sublattice in $Yb_2V_2O_7$ and $Tm_2V_2O_7$ it is necessary to account for the behavior of the vanadium sublattice. Since the critical temperature appears independent of the *RE*, the vanadium–vanadium interaction is assumed to be constant over the three pyrochlores.

TABLE I

	Ground term of *RE*	T_c (K)	Saturation expt (4K)	Calc[a] moment (μ_B/molecule)	a_0 (Å) (7)
$Lu_2V_2O_7$	$^1S_0$	74.6(4)	1.86(10)	2.0	9.928(2)
$Yb_2V_2O_7$	$^2F_{7/2}$	73.2(4)	5.42(10)	10.0	9.948(1)
$Tm_2V_2O_7$	$^3H_6$	71.4(4)	2.43(10)	16.0	9.973(1)

[a] Assumes *RE* free ion moment, a spin-only moment for V^{4+}, and ferromagnetic coupling.

It can therefore be determined directly from $Lu_2V_2O_7$ where Lu^{3+} is an $^1S_0$ ion. Molecular field theory treats the problem of two interpenetrating sublattices by assuming that an average internal field is generated which may be represented by

$$H_M^V = \lambda_{VV} M_V + \lambda_{RV} M_R,$$

$$H_M^R = \lambda_{RV} M_V + \lambda_{RR} M_R.$$

λ_{VV} and λ_{RR} represent the intrasublattice coupling in the vanadium and rare earth sublattices and λ_{RV} the intersublattice coupling. M_V and M_R are the magnetizations of the two sublattices. Since the critical temperatures of the vanadium pyrochlores are almost independent of *RE* and $Yb_2Ti_2O_7$ (Ti^{4+} is d^0) does not order down to 4K (5), λ_{RR} was assumed to be negligible and λ_{RV} small compared to λ_{VV}. The molecular fields were then simplified to

$$H_M^R = \lambda_{RV} M_V,$$

$$H_M^V = \lambda_{VV} M_V.$$

All the data for $Yb_2V_2O_7$ and the $T > T_c$ data for $Tm_2V_2O_7$ were treated using the assumption that the vanadium contribution could be subtracted directly, leaving only the molecular field $\lambda_{RV} M_V$ as an adjustable parameter. The paramagnetic susceptibility per *RE* ion was therefore calculated using

$$2\chi_{EXP}^{RE}(T) = \frac{M_{TOTAL} - M_{Lu_2V_2O_7}}{H_{EXT} + \lambda_{RV} M_V}. \quad (1)$$

A different procedure was necessary for $Tm_2V_2O_7$ at $T < T_c$ because $M(Tm_2V_2O_7) - M(Lu_2V_2O_7)$ values were small, therefore experimental errors dominated. Furthermore, it was difficult to estimate $M(Tm_2V_2O_7)$ because of the slope of the M versus H curves, even at 4K. Close examination of these curves, some of which are shown in Fig. 3, showed a linear high field region. The slope $(\partial M/\partial H)_T$ was interpreted as χ_{Tm} directly. As seen from the $Lu_2V_2O_7$ data, χ_V was almost zero at low temperatures, however, near T_c it was necessary to subtract a contribution caused by the vanadium sublattice. This procedure also provided an independent estimation of λ_{RV} because $\chi_{Tm} = M_{Tm}/\lambda_{RV} M_V$. For the low-temperature $Tm_2V_2O_7$ values it was necessary to estimate and subtract a diamagnetic susceptibility. When Eq. (1) was used the diamagnetic contribution is removed by the subtraction of $M(Lu_2V_2O_7)$.

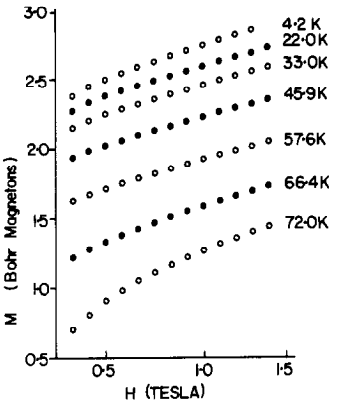

FIG. 3. Magnetic moment, per $Tm_2V_2O_7$, versus field curves taken at various temperatures. The slopes of these curves were used to determine the Tm^{3+} susceptibility.

Calculated Susceptibilities

The experimental susceptibility data were interpreted by fitting to a theoretical model, using the van Vleck formalism

$$\chi^{RE}_{\text{THEO}} = \frac{N_0 g_J^2 \mu_B^2}{kTZ} \sum_i \left[|\langle\psi_i|\bar{\mu}|\psi_i\rangle|^2 - 2\sum_{j\neq i} \left| \frac{\langle\psi_i|\bar{\mu}|\psi_j\rangle}{E_i - E_j} \right|^2 kT \right] e^{-E_i^0/kT},$$

$$Z = \sum_i e^{-E_i^0/kT}, \quad (2)$$

where g_J is the free ion gyromagnetic ratio. The first-order matrix element represents the Zeeman splitting while the second-order term is the temperature-independent van Vleck susceptibility arising from states mixing in a magnetic field. The E_i^0's represent the splittings resulting from the crystalline electric field.

The eigenfunctions and eigenvalues were obtained using perturbation theory. In the case of the rare earths, the splitting of the free ion term, caused by spin–orbit coupling, is considered a larger perturbation than the crystal field, so the Hamiltonian may be written

$$\mathcal{H}_{RE} = \mathcal{H}_{\text{FREE ION}} + \mathcal{H}_{\text{CEF}} - \bar{\mu} \cdot \bar{H},$$

where $\mathcal{H}_{\text{FREE ION}}$ includes spin–orbit coupling. Since the site symmetry of the *RE* is D_{3d} the crystal field Hamiltonian is

$$\mathcal{H}_{\text{CEF}} = B_2^0 O_2^0 + B_4^0 O_4^0 + B_4^3 O_4^3 + B_6^0 O_6^0 + B_6^3 O_6^3 + B_6^6 O_6^6.$$

Cubic site symmetry was assumed in order to limit the number of adjustable parameters.

The Hamiltonian used was

$$\mathcal{H}_{\text{CEF}} = B_4^0[O_4^0 - 20\,2^{1/2} O_4^3] + B_6^0[O_6^0 + 35\,2^{1/2}/4\,O_6^3 + 77/8\,O_6^6],$$

where the trigonal axis is chosen as the z axis. The O_n^m's are the Stevens operator equivalents (*8*) which are tabulated (*9*) for each free ion state and the B_n^m's are the crystal field coefficients. Initial values of B_n^m's were obtained from nearest-neighbor point charge calculations. The Hamiltonian was diagonalized to obtain eigenvectors and energy spacings, the susceptibilities were calculated, and this procedure was iterated to obtain the best fit. Comparisons of experimental and calculated susceptibilities are shown in Figs. 4 and 5.

The possible energy level separations, in the case of cubic symmetry, can be characterized by two parameters, an energy scaling and a ratio of the fourth- to sixth-order crystal field terms. Lea *et al.* (*10*) related these to two parameters W and X, which

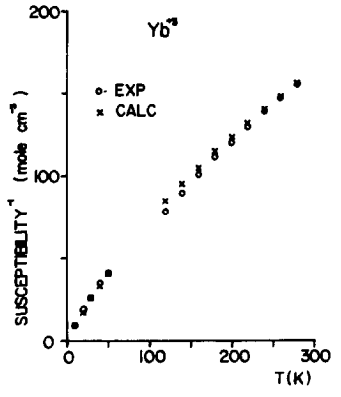

FIG. 4. A comparison of the calculated and experimental inverse susceptibilities for Yb^{3+}. The critical temperature is 73.2K.

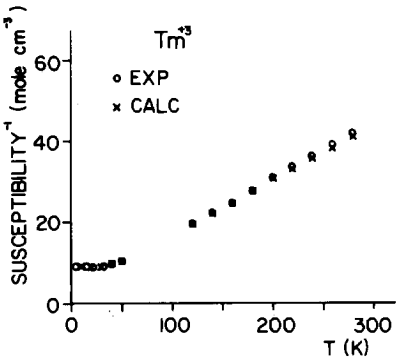

FIG. 5. A comparison of the calculated and experimental inverse susceptibilities for Tm^{3+}. The critical temperature is 71.4K.

they plotted for different f-electron terms. These plots proved very useful as a check of the computer diagonalization procedure. The results are shown in Table II.

Discussion

Yb^{3+}, a Kramers ion with a $^2F_{7/2}$ ground term, is expected to split into two doublets and a quartet in a cubic crystal field. The best fit to the data places the Γ_7 doublet as the ground state with the quartet Γ_8 1100K above the ground state and $E_{\Gamma_6}-E_{\Gamma_7}$ at approximately 1800 K.

Attempts were also made to fit the Yb^{3+} data to the axial Hamiltonian chosen by Dunlap *et al.* (*5*). The magnetization versus temperature data, below T_c, fit well to an axial model with $|\pm\frac{3}{2}\rangle$ as the ground state and $E|\frac{1}{2}\rangle - E|\frac{3}{2}\rangle = 37$K. This is in reasonable agreement with Dunlap's splitting of 18K. However, this axial model could not be reconciled with the higher-temperature data, where it predicted free ion behavior.

The axial and cubic models both predict a ground state moment of 1.7 μ_β, in agreement with 4-K saturation magnetization as well as neutron diffraction (*3*) and Mössbauer (*11*) data.

Tm^{3+}, with a $^3H_6$ ground term, has an even number of electrons and, in a cubic crystal field, is split into three triplets, a doublet, and two singlets. The energy level ordering obtained from the fitting procedure is shown in Fig. 6. The temperature independence of the low-temperature data is accounted for by a ground state singlet, Γ_2, with a tripled, Γ_5, 140K above the ground state.

TABLE II

	Tm^{3+}	Yb^{3+}	Yb^{3+} in $Yb_2Ti_2O_7$ (*6*)
W	−4.114	60	—
X	0.65	0.95	—
λ_{RV}[a]	2.5	14	—
B_4^0 (K)[b]	0.0297	−0.633	−0.498
B_6^0 (K)	−0.000339	0.000705	0.000719
$A_4^0\langle r^4\rangle$ (K)	170	380	300
$A_6^0\langle r^6\rangle$ (K)	16.6	1.53	1.56

[a] λ in units of moles of vanadium ions per cm^3.

[b] These values are based on the threefold axis as the z axis. The conversions to the B's used by Lea *et al.* (*10*) are $B_4^{0(LLW)} = -\frac{1}{2}B_4^0$, $B_6^{0(LLW)} = \frac{8}{16}B_6^0$.

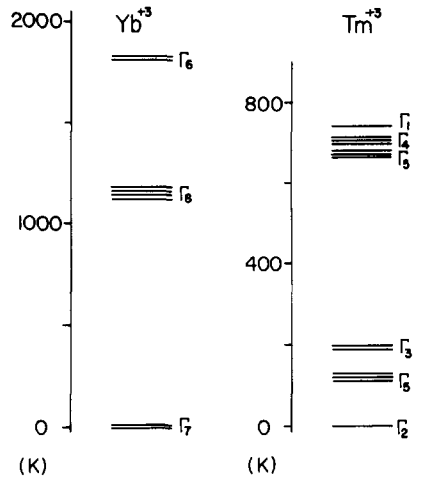

FIG. 6. Calculated energy level diagrams for Yb^{3+} and Tm^{3+}.

Values of the coupling constants λ_{RV}, in terms of moles of vanadium ions, were determined to be 14 mole cm^{-3} for Yb^{3+} and 2.5 mole cm^{-3} for Tm^{3+}. These values can be compared to 580 mole cm^{-3} obtained for λ_{VV} from the mean field expression for the critical temperature

$$T_c = (\mu\lambda_{VV}M_V)/3k.$$

These results support the argument that the vanadium sublattice is the driving force for the magnetic ordering.

The B_n^m's can be rewritten as $B_n^m = A_n^m\langle r^n\rangle\theta_n$. The $\langle r^n\rangle$'s are expectation values over the $4f$ orbitals (*12*) and θ_n's are reduced matrix elements (*9*) usually designated α, β, γ for $n = 2,4,6$. A_n^m's depend only on the rare earth environment and should be independent of the lanthanide ion. Dunlap and Shenoy (*13*) fit susceptibilities in a series of cryolites Cs_2NaRCl_6,

where R is a rare earth ion in cubic site symmetry, and found the A_n^m's were indeed invariant to the RE ion, to within experimental error.

The comparison of A_n^m for Tm^{3+} and Yb^{3+} in the vanadium pyrochlores shows a discrepancy in the A_4^0 terms with the most probable cause the deviation of the site from cubic symmetry. The Yb^{3+} quartet at 1100K is split into two doublets in D_{3d} symmetry, but this does not significantly alter the calculated susceptibility because of the larger energy denominator in the second-order term in Eq. (2). Furthermore, rediagonalization of the crystal field Hamiltonian with an added B_2^0 term of 13K alters the ground state moment by less than 2%. Similar results were found for Yb^{3+} in gallium and aluminum garnets (*14*). However, this is not the case with Tm^{3+}, which has an excited state triplet at 140K above the ground state which will split into a singlet and a doublet in lower symmetry. The B_2^0 term here could play an important role in the susceptibility, even at low temperatures. Calculation of the splitting in noncubic symmetry also relaxes the fourth and sixth-order relationships. It was felt that the magnetic data did not justify the inclusion of the three extra terms in the Hamiltonian.

Conclusions

The pyrochlores $(RE)_2V_2O_7$ (RE = Tm, Yb) were treated as an interpenetrating ferromagnetic vanadium sublattice and a weakly coupled RE sublattice. For the RE sublattice cubic crystal field Hamiltonian was adjusted to obtain an energy level scheme which was used to calculate magnetic susceptibilities. The energy level diagram obtained for $Yb_2V_2O_7$ was similar to one obtained by Townsend and Crossley (*6*) for the isostructural compound $Yb_2Ti_2O_7$.

Acknowledgments

We wish to thank G. Hewitson for his invaluable technical assistance and Dr. M. F. Collins for helpful discussions. We also acknowledge C. W. Turner and J. F. Britten for computing advice. This work was supported by the National Sciences and Engineering Research Council of Canada. One of us (L.S.) wishes to acknowledge the financial support of an Ontario Graduate Scholarship.

References

1. G. V. Bazuev, O. V. Makarova, V. Z. Oboldni, and G. P. Shveikin, *Akad. Nauk. SSSR* **230,** 869 (1976).
2. G. V. Bazuev, A. A. Samokhvalov, Y. N. Morozov, I. I. Matveenko, V. S. Babushkin, T. I. Arbuzova, and G. P. Shveikin, *Sov. Phys. Solid State* **19,** 1913 (1977).
3. L. Soderholm, J. E. Greedan, and M. F. Collins, *J. Solid State Chem.* **35,** 385 (1980).
4. T. Shin-ike, G. Adachi, and J. Shiokawa, *Mater. Res. Bull.* **12,** 1149 (1977).
5. B. D. Dunlap, G. K. Shenoy, J. M. Friedt, M. Meyer, and G. J. McCarthy, *Phys. Rev.* **18,** 1936 (1978).
6. M. G. Townsend and W. A. Crossley, *J. Phys. Chem. Solids* **29,** 593 (1968).
7. J. E. Greedan, *Mater. Res. Bull.* **14,** 13 (1979).
8. K. W. H. Stevens, *Proc. Roy. Soc. London Ser. A* **1952,** 209 (1952).
9. M. T. Hutchings, *Solid State Phys.* **16,** 227 (1964).
10. K. R. Lea, M. J. M. Leask, and W. P. Wolf, *J. Phys. Chem. Solids* **23,** 1381 (1962).
11. L. Soderholm and J. E. Greedan, unpublished data.
12. A. J. Freeman and R. E. Watson, *Phys. Rev.* **127,** 2050 (1962).
13. B. D. Dunlap and G. K. Shenoy, *Phys. Rev. B* **12(7),** 2716 (1975).
14. J. J. Pearson, G. F. Herrmann, K. A. Wickershiem, and R. A. Buchanan, *Phys. Rev.* **159(2),** 251 (1967).